ESM Roughness Datasets (ARC)

Michael C. Wilder
Aerothermodynamics Branch, NASA Ames Research Center

NASA STMD/ECF Workshop - Hypersonic Transition and Turbulence Modeling: Part 1, July 8, 2024

Motivation

- Thermal Protection System (TPS) materials used on atmospheric entry vehicles have surface roughness characteristic of the material and fabrication methods
- Surface roughness can evolve in response to ablation and other mechanisms that occur during exposure to the flight environment
- The roughness can affect the boundary layer state, and can lead to significant increases in heating rates

Artist's Rendering of Galileo Probe at Jupiter

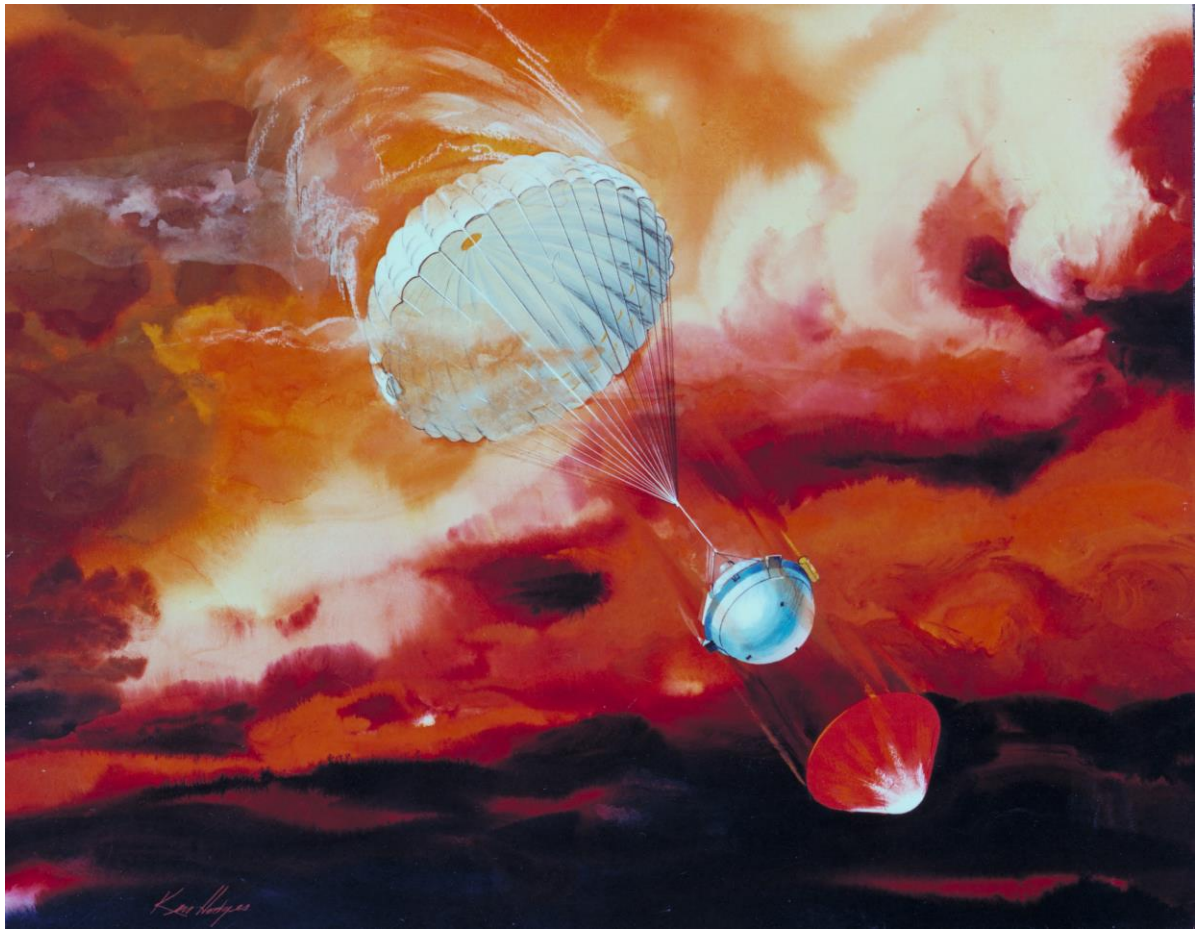

NASA Artwork by Ken Hodges

Woven TPS: HEEET and 3MDCP

- This work focused on the effects on turbulent heat transfer due to surface roughness of types relevant to NASA entry missions, and was supported by NASA's Entry Systems Modeling (ESM) Project
- The emphasis was on new classes of woven materials, which are enabling for many missions
  - Heatshield for Extreme Entry Environment Technology (HEEET)
  - 3-D Medium Density Carbon Phenolic (3MDCP)*
    - Single-layer TPS derivative of the HEEET insulation layer

HEEET Engineering Test Unit

Cross Section of Dual-Layer HEEET

Recession Layer (RL)
- **Densely woven carbon fibers**

Insulation Layer (IL)
- **Looser weave of carbon and phenolic yarns**

*Ellerby, D., et al. (2021). TPS and Entry Technologies for Future Outer Planet Exploration. Bulletin of the AAS, 53(4). https://doi.org/10.3847/25c2cfeb.9453cc81

Introduction

- HEEET was characterized using 3D surface scans of material samples before and after ablation under turbulent flow conditions

Arcjet-Ablated HEEET Sample*

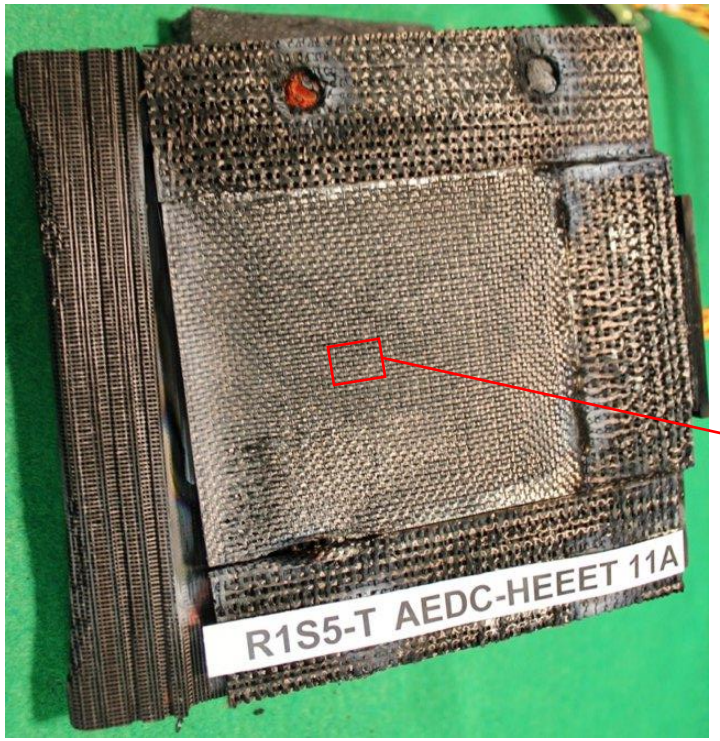

Pre-Test Measurement

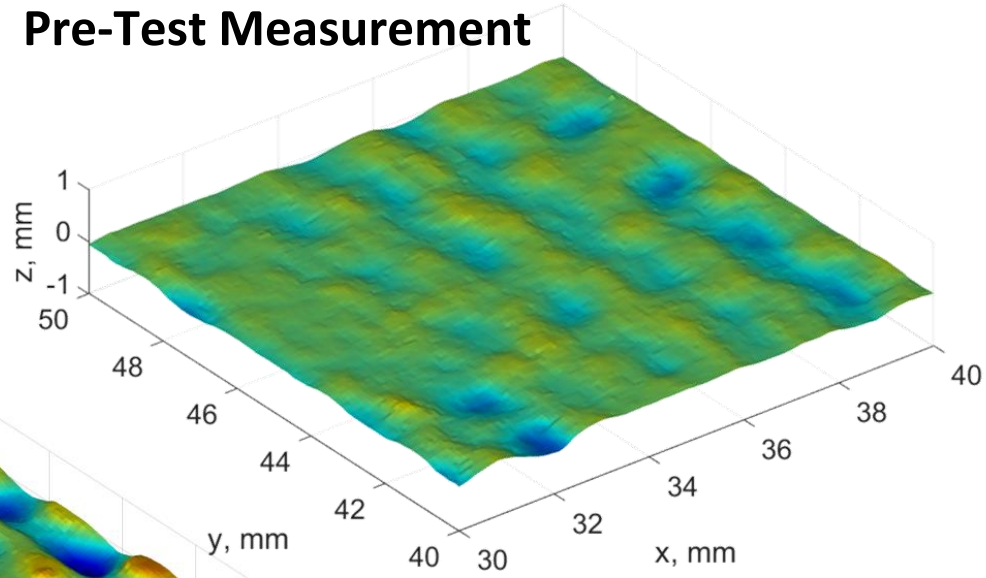

Post-Test Measurement

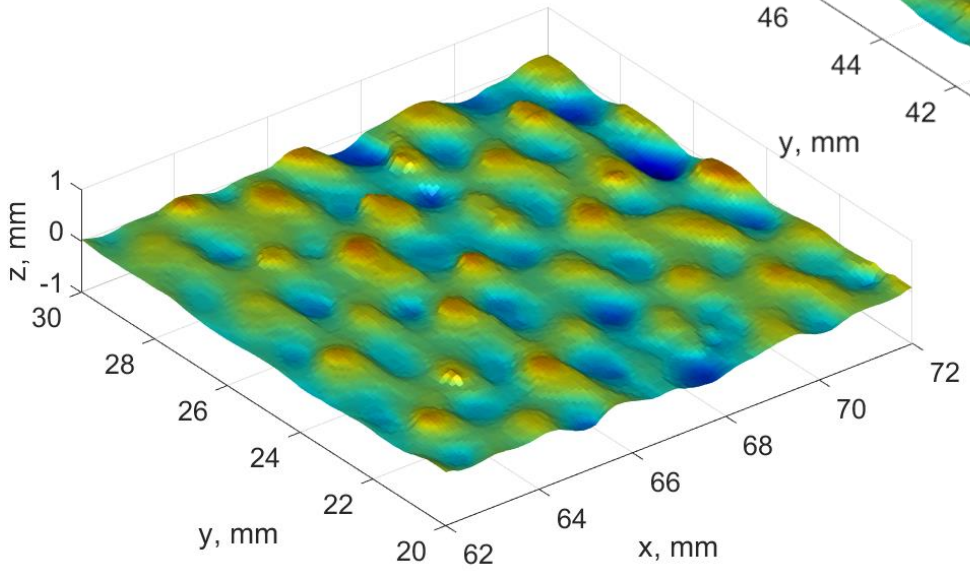

*Venkatapathy, E., *et al.*, "TPS for Outer Planets," Outer Planets Assessment Group (OPAG) Technology Forum; 21-22 Feb. 2018

Model Patterns

The Woven pattern was idealized as a combination of sinusoidal function to give an eggcrate-like pattern

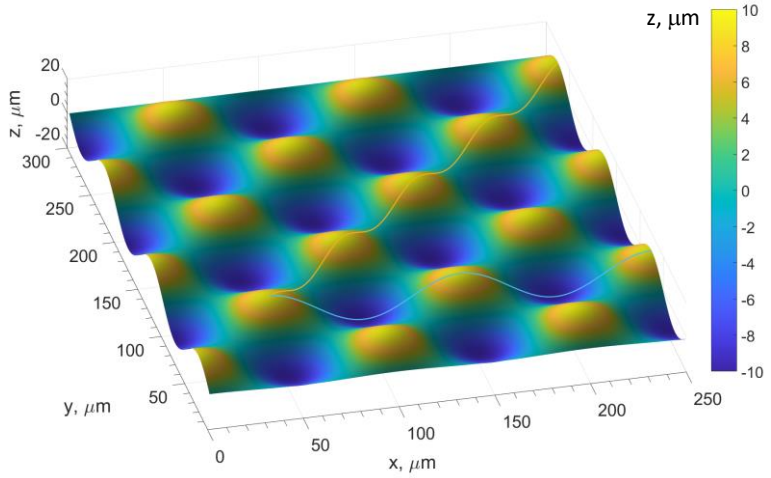

Example of a ballistic-range model pattern as-built

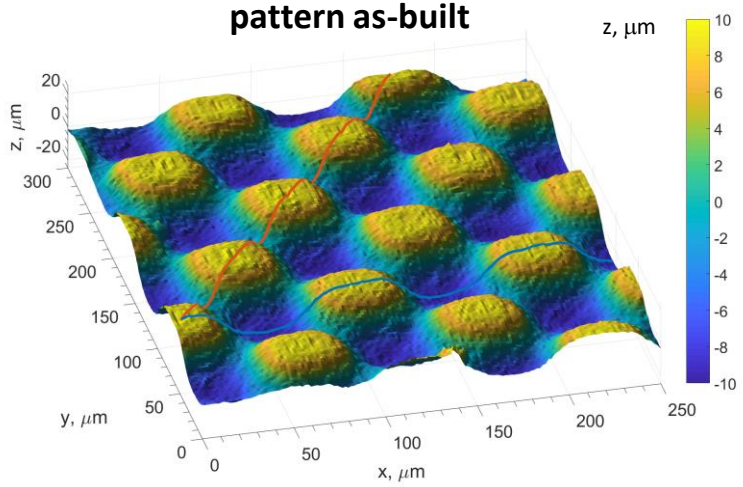

The as-built ballistic-range roughness elements tended to be

- Slightly more blunt than the idealized pattern or the ablated HEEET material

HEEET also has two different wavelengths (not modeled in the ballistic-range tests)

- a factor of how the material is woven
- Ballistic-range models matched the peak-to-valley wavelength

Ballistic-range model compared with the idealized patten

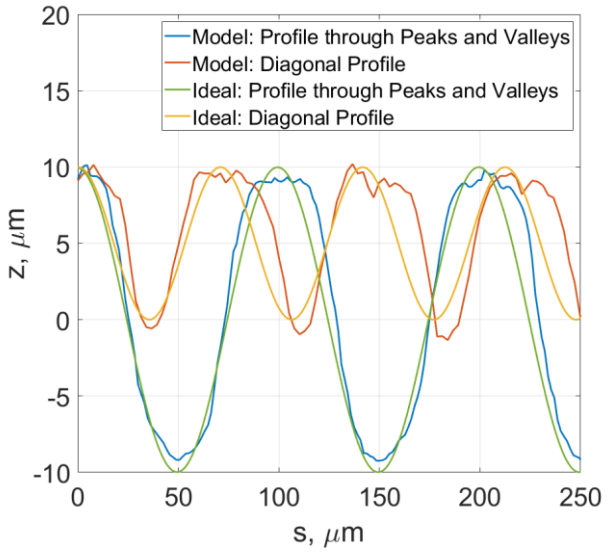

Ballistic-range model compared with Ablated HEEET

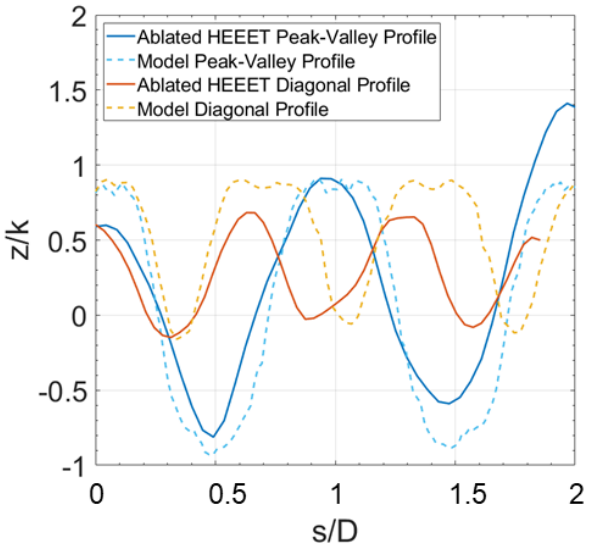

Model Patterns

Three basic patterns

- RL, representing the ablated HEEET recession layer scaled from a 0.76 m diameter vehicle* to the 30.48 mm diameter ballistic-range model
  - Three height variants were tested, 10, 20, and 40 μm
- IL, representing the ablated HEEET insulation layer (3MDCP) as a 2x scale-up of the RL pattern.
- PO, a variant of the IL patterns having only peaks.
  - Meant to represent a pattern similar to those tested by Schlichting** having protuberances on an otherwise flat surface. The pattern differs from the Schlichting layout.

RL Pattern
Nominal element height = 20 μm

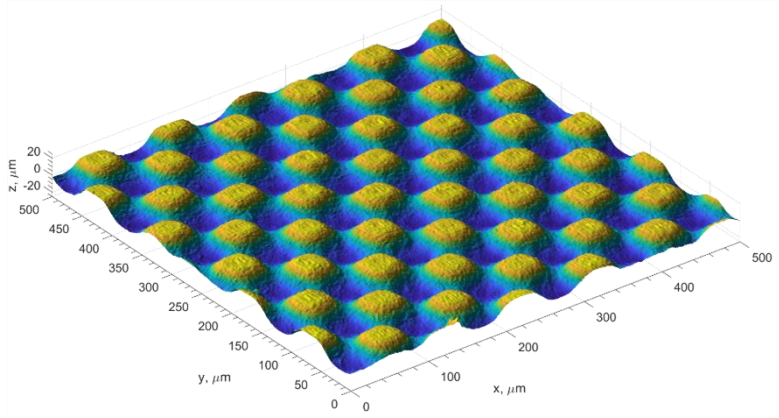

IL Pattern
Nominal element height = 40 μm
Nominal element spacing = 2x RL spacing

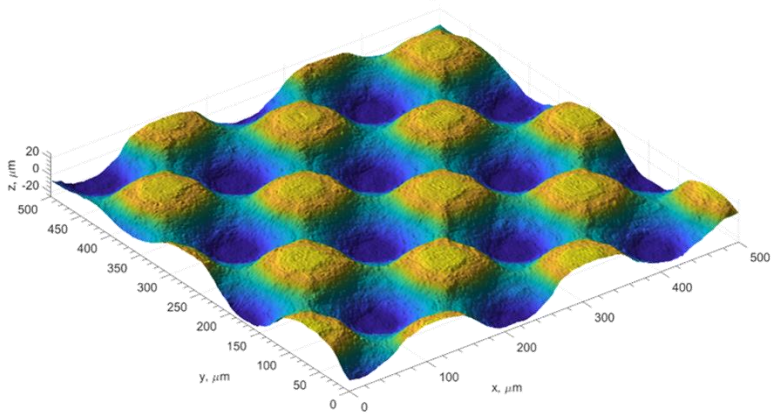

PO Pattern
IL Pattern with only the peaks
Nominal element height = 20 μm

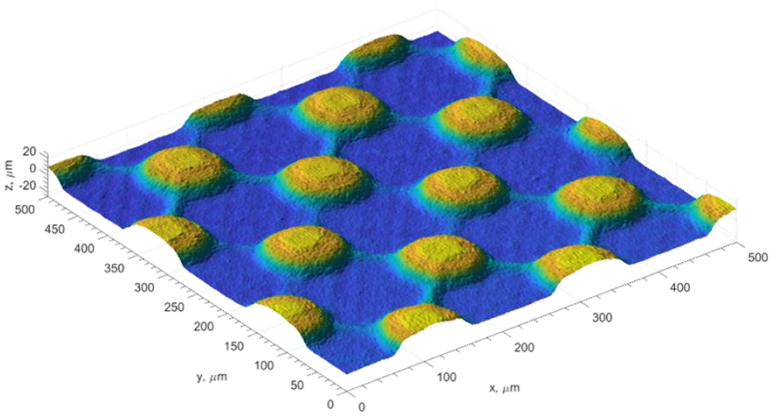

*Palmer, et al., AIAA 2013-2776
**Schlichting, NACA-TM-823, 1937

Model Patterns: RL height varients

Half-Height Pattern
Nominal element height = 10 μm

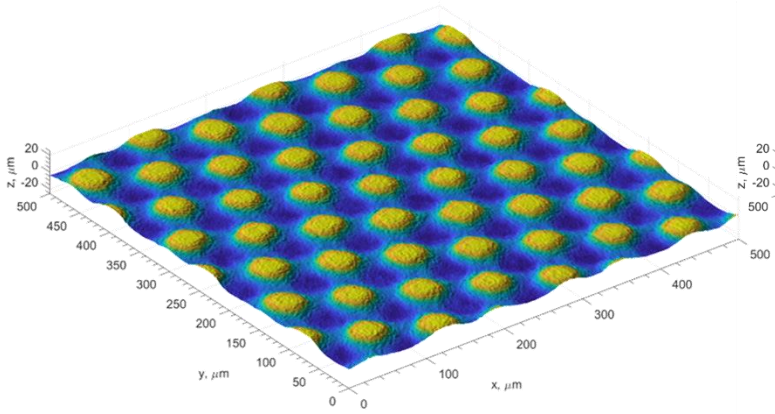

"Ablated-Height" Pattern
Nominal element height = 20 μm

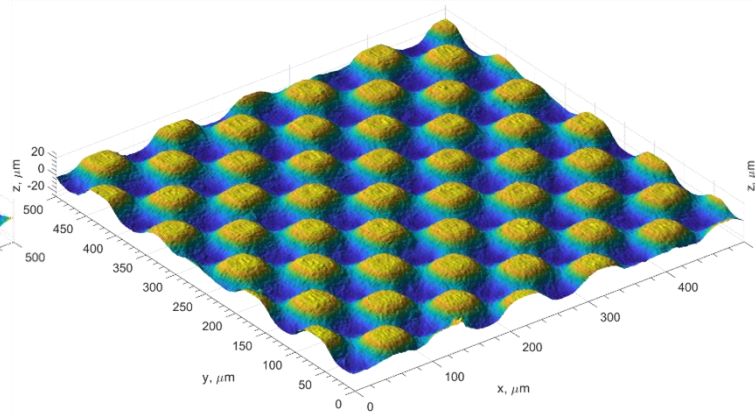

Double-Height Pattern
Nominal element height = 40 μm

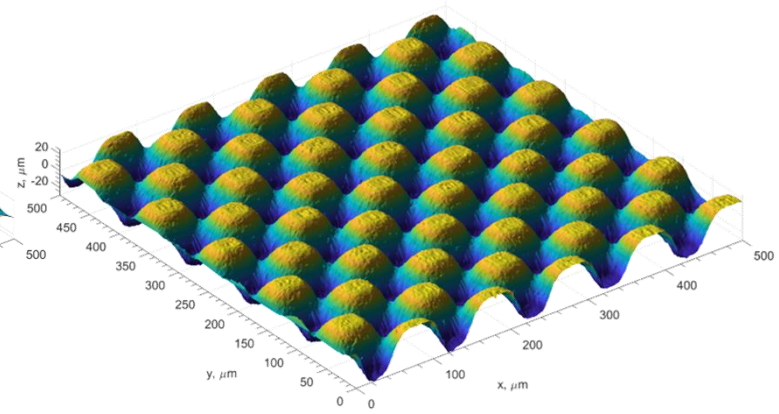

Model Patterns: Roughened Patterns

Roughened patterns were also assessed to better represent an ablated surface.

Roughened 20 μm RL Patterns:

Roughened with 400-grit AlOx
Average particle size = 22 μm

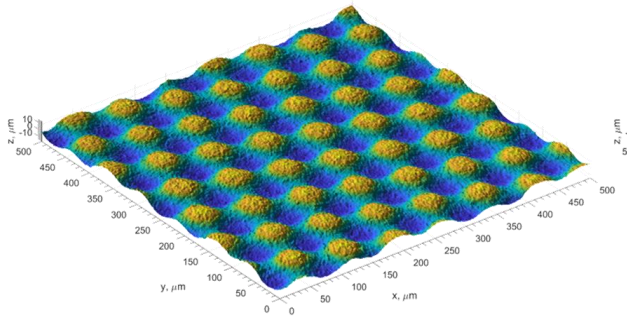

Roughened with 220-grit AlOx
Average particle size = 63 μm

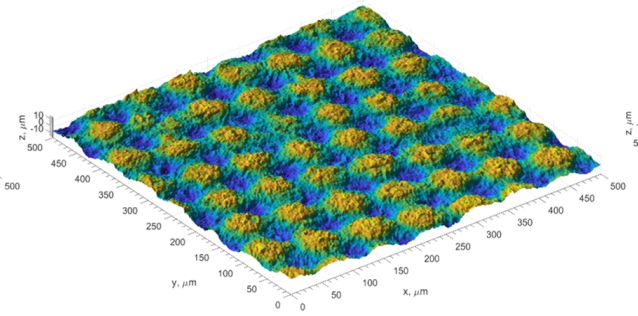

Roughened with B120 microspheres
Average particle size = 102 μm

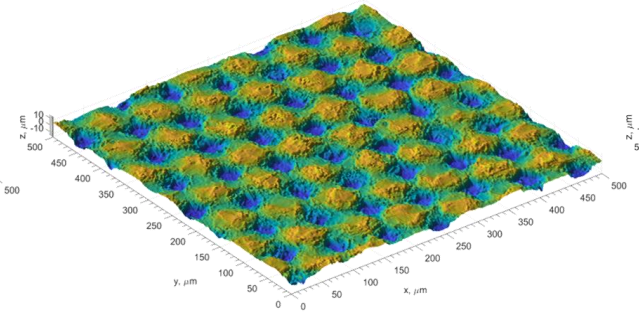

Roughened with 120-grit AlOx
Average particle size = 102 μm

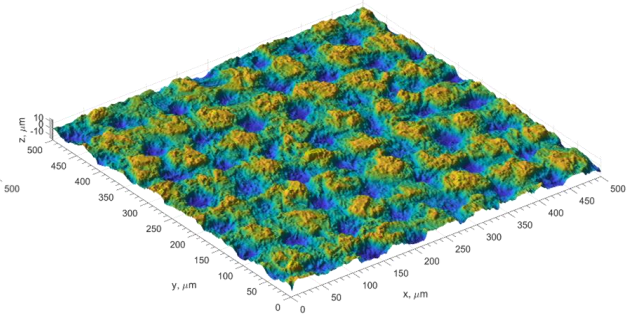

Roughened 40 μm RL Patterns :

Roughened with 400-grit AlOx
Average particle size = 22 μm

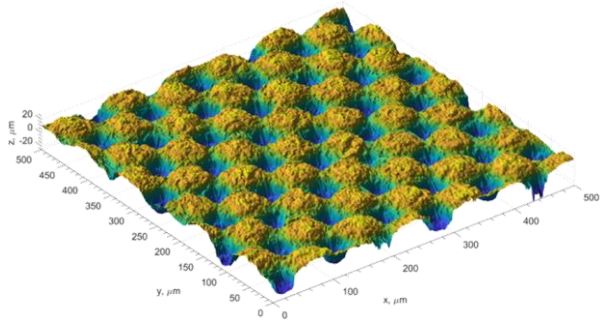

Roughened with 220-grit AlOx
Average particle size = 63 μm

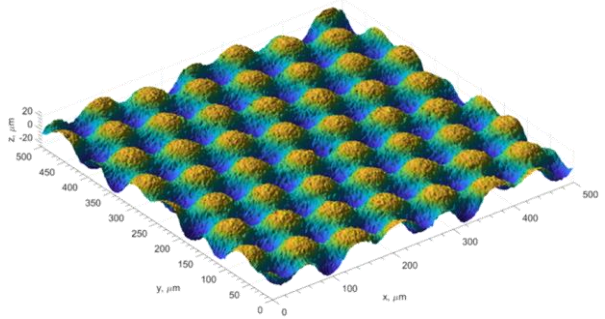

Roughened with 120-grit SiC
Average particle size = 102 μm

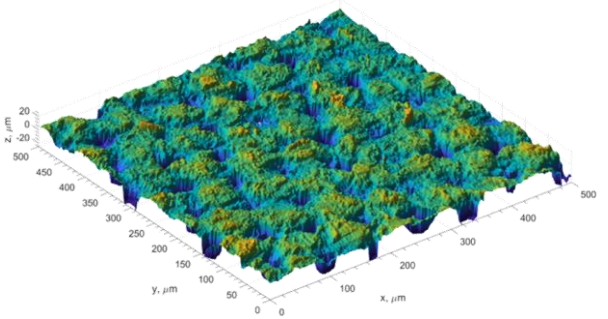

Model Patterns: Roughened Patterns

Roughened patterns were also assessed to better represent an ablated surface.

Roughened IL Patterns:

Roughened with 400-grit AlOx
Average particle size = 22 μm

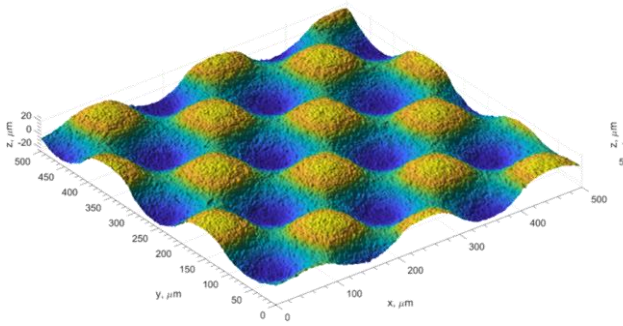

Roughened with 220-grit AlOx
Average particle size = 63 μm

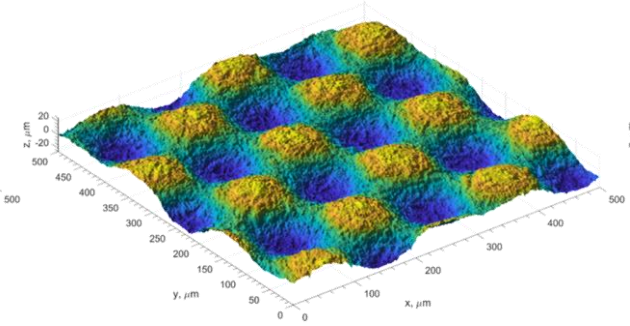

Roughened with B120 microspheres
Average particle size = 102 μm

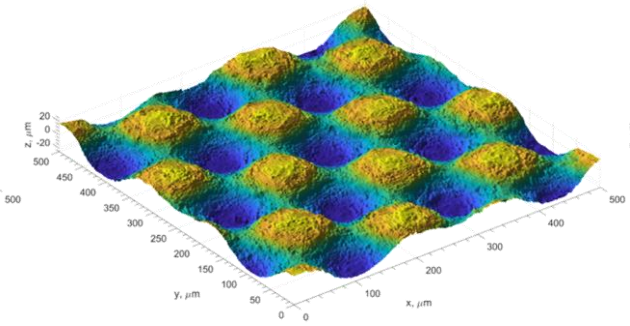

Roughened with 120-grit AlOx
Average particle size = 102 μm

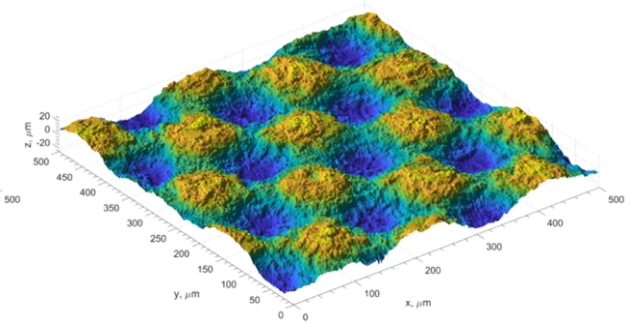

Grit-Blast Roughness

Each ballistic-range model also had a sandgrain-like roughness produced by grit-blasting:

Roughened with 400-grit AlOx
Average element height = 2.4 μm

Roughened with B120 microspheres
Average element height = 2.5 μm

Roughened with 220-grit AlOx
Average element height = 5.7 μm

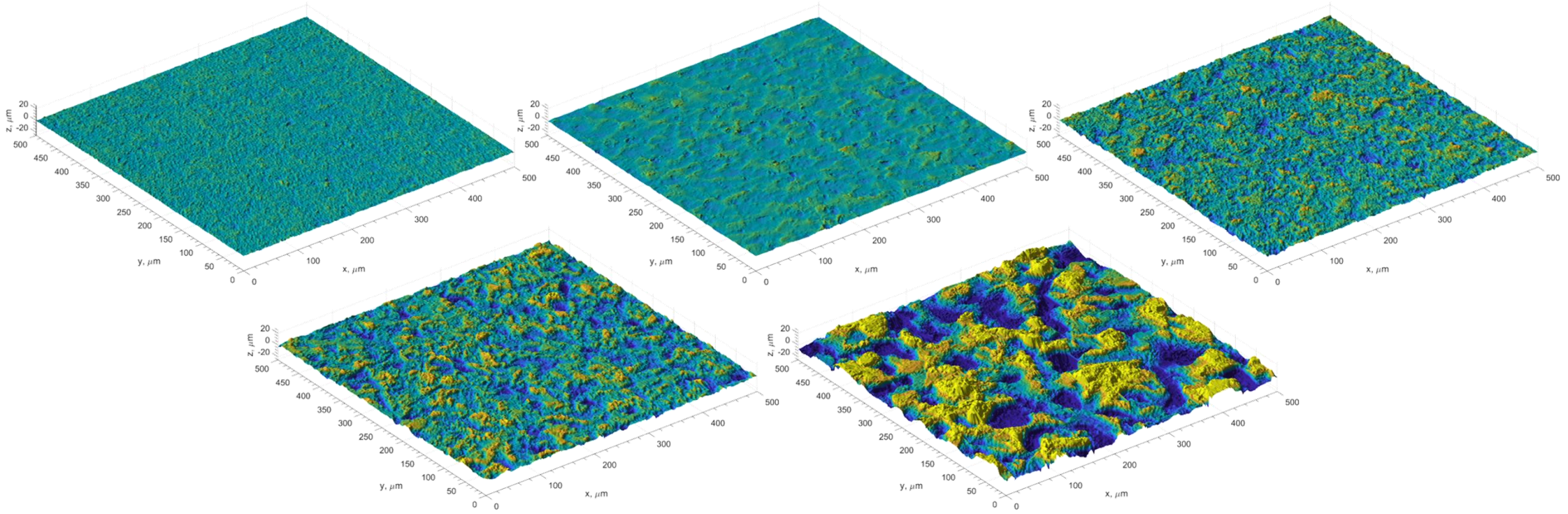

Roughened with 120-grit AlOx
Average element height = 6.6 μm

Roughened with 60-grit SiC
Average element height = 19.4 μm

Model Geometry and Texture Layouts

The Models were 45° Sphere-Cones

- Base diameter = 30.48 mm, Nose radius = 7.62 mm (0.5 Base radius)
- The nose cap was roughened by grit-blasting in order to trip the flow
- Each model had at least two surface textures, plus smooth-wall segments, as shown below
- Heat flux was averaged circumferentially through a given surface texture area, and axially over $1.55 \le s/R_n \le 1.85$

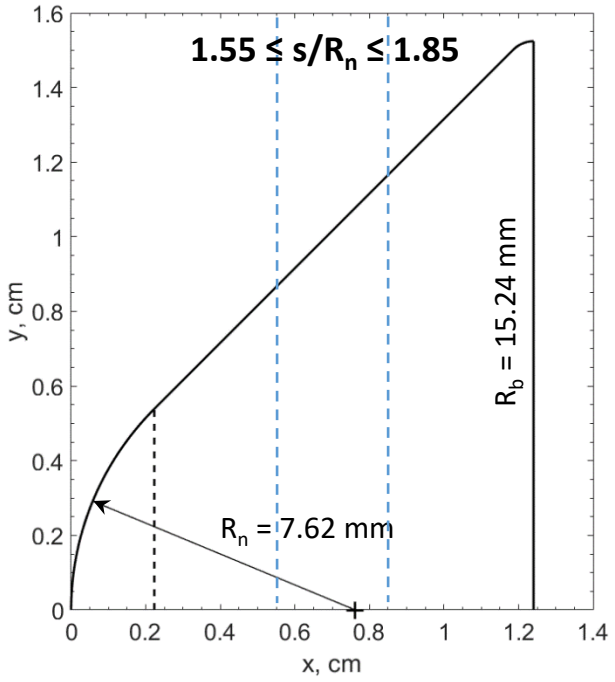

Model with One Pattern Segment and Two Girt-Blasted Segments

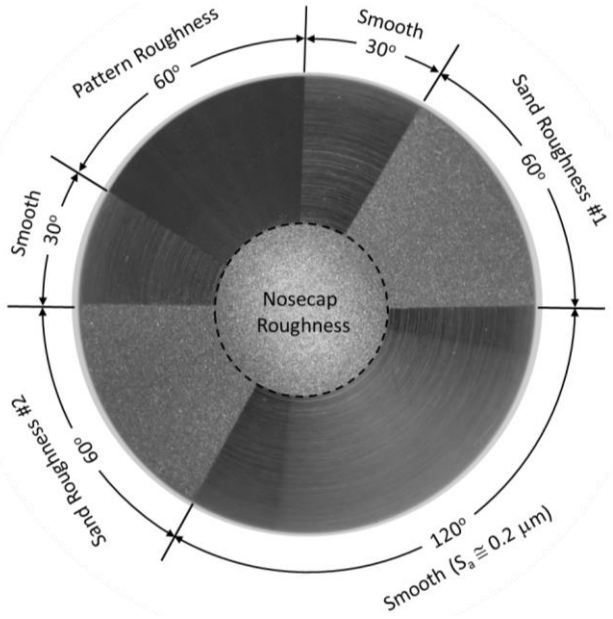

Model with Two Pattern Segments

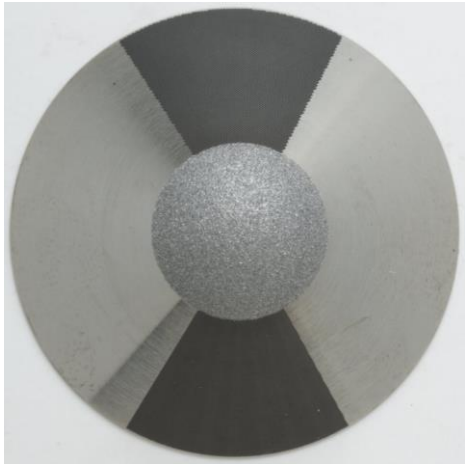

Model with Two Pattern Segments, Two Roughened Pattern Segments, and Two Girt-Blasted Segments

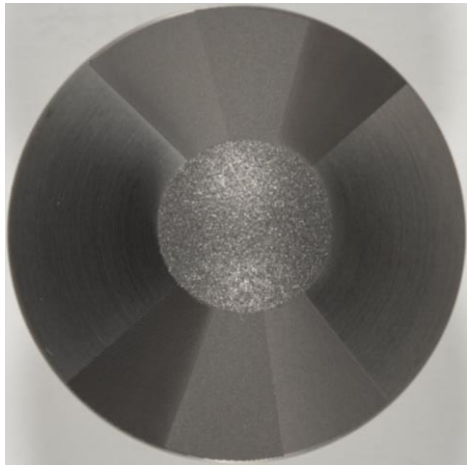

Test Facility

- **Hypervelocity Free Flight Aerodynamic Facility (HFFAF)**
  - Gun-launched, free-flight facility
  - Tests were in air at pressures from 0.15 atm to 0.3 atm
  - Launch speeds between 3.2 km/s to 3.5 km/s (mid-range from 2.7 km/s to 3.3 km/s)
  - Roughness Reynolds numbers (based on roughness height) from ~10 to ~300
  - Stagnation cold-wall heat flux from ~3000 W/cm^2 to ~5000 W/cm^2

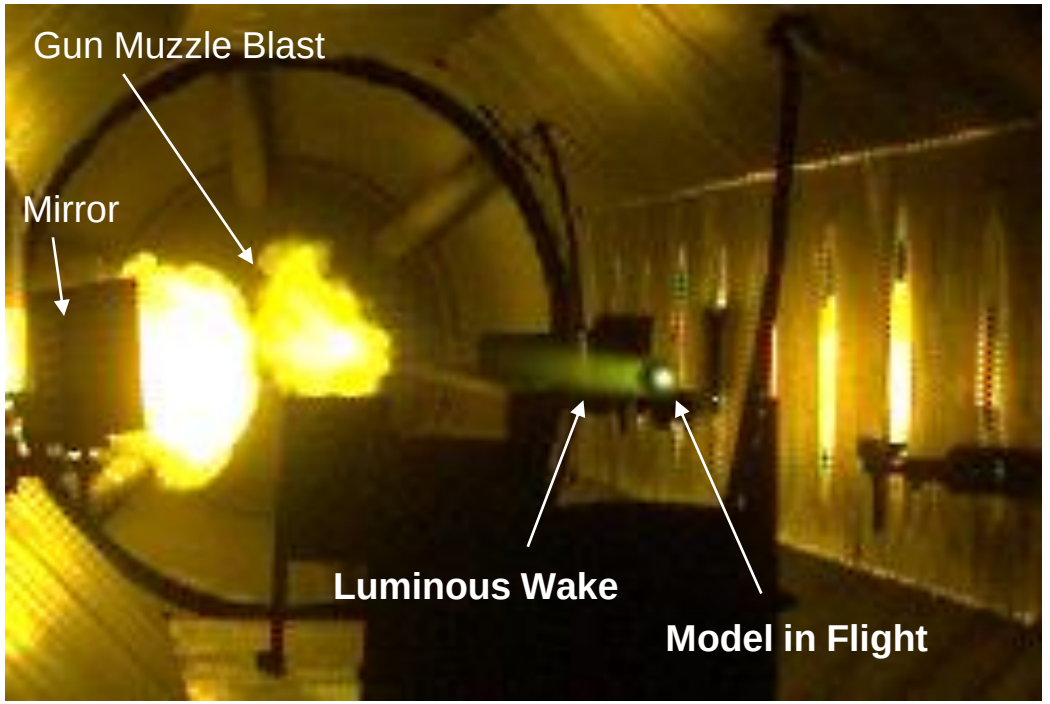

Test Conditions

- Test Conditions
  - Five basic test conditions to provide a range of roughness Reynolds numbers
  - Ti-6Al-4V for all condition but Condition 4, which used 304 Stainless Steel models
  - Condition 1: 13 shots, all surface textures tested.
  - Condition 2: 7 shots, IL, RL20 and RL40, plus roughened varieties of all three
  - Condition 3: 1 shot (off-nominal Condition 4 shot) with IL and PO textures
  - Condition 4: 3 shots, IL, RL10, and RL20
  - Condition 5: 1 shot, IL and PO

Launch Conditions			Conditions at mid range, at s/Rn = 1.7, Smooth-Wall Turbulent CFD													
Condition	**Launch V, m/s**	**q_{stag}, W/cm^2**	**V, m/s**	**P, atm**	**ρ_∞, kg/m^3**	**q_w, W/cm^2**	**T_{ws}, K**	**T_e, K**	**h_{ws}, J/kg**	**h_e, J/kg**	**M_e**	**Re_θ**	**θ, μm**	**δ, μm**	**δ^*, μm**	**δ_s, μm**
1	3222	3094	2988	0.15	0.1765	1742	650	3151	7.52E+05	4.75E+06	1.16	44.71	33.33	217.20	25.80	2.59
2	3500	4538	3222	0.20	0.2353	2601	750	3365	6.64E+05	5.17E+06	1.21	38.05	29.03	190.29	25.17	1.85
3	3222	3950	2800	0.25	0.2942	1903	750	2896	5.15E+05	3.90E+06	1.15	45.90	27.08	182.54	21.58	2.23
4	3429	4873	3222	0.25	0.2942	3125	650	3385	5.64E+05	5.17E+06	1.19	42.23	27.46	181.97	22.74	1.41
5	3222	4285	2700	0.30	0.3530	1929	750	2758	4.92E+05	3.63E+06	1.13	44.59	25.72	177.42	20.68	2.05

Test Approach

Muzzle: **Diaphragm Rupture** **Launch** **2.1 m from Muzzle: Sabot Separation** **Shadowgragh**

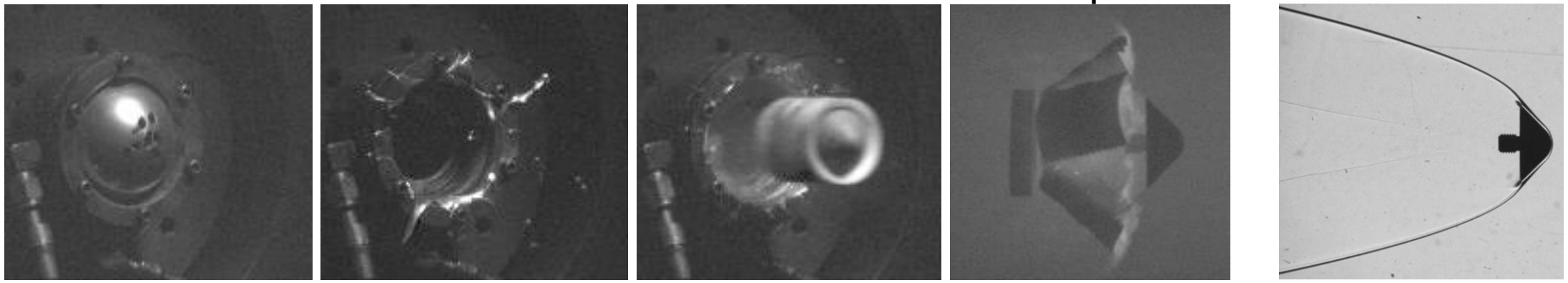

Example IR images:

2-Textured Model

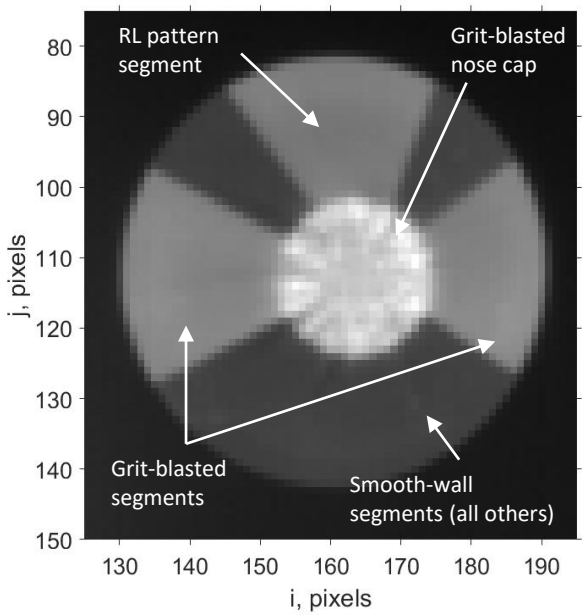

5-Textured Model

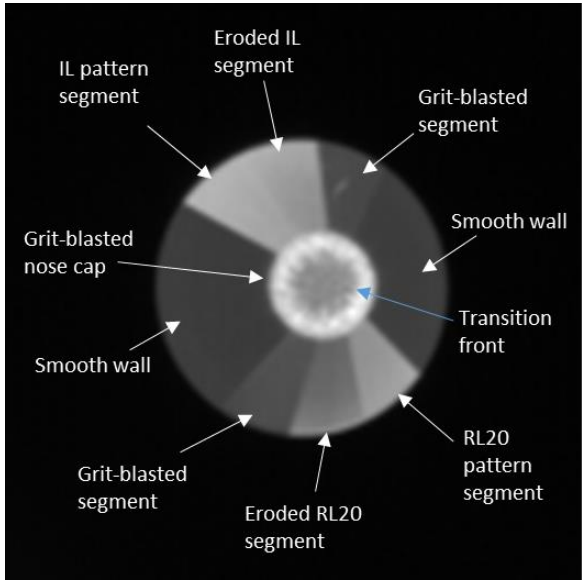

Test Approach

- Surface temperature of the projectile is measured using mid-wave IR cameras
- The inverse heat conduction problem is solved from the measured surface temperatures given the temperature-dependent thermal properties of the model material
  - Details can be found in AIAA-2011-3476

Example of Model with Grit-Roughened Surface*

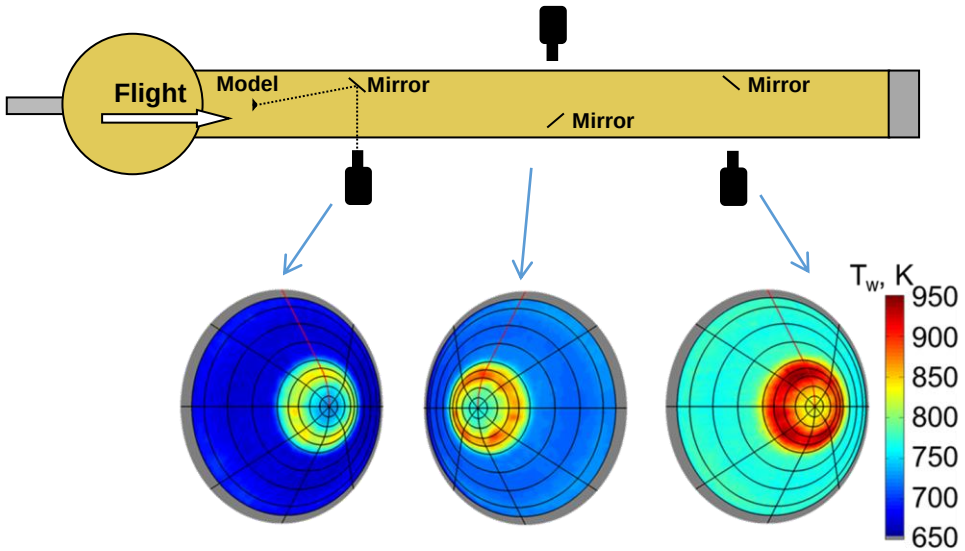

*AIAA 2014-0512

Stagnation-Point Heat Flux on Hemispheres

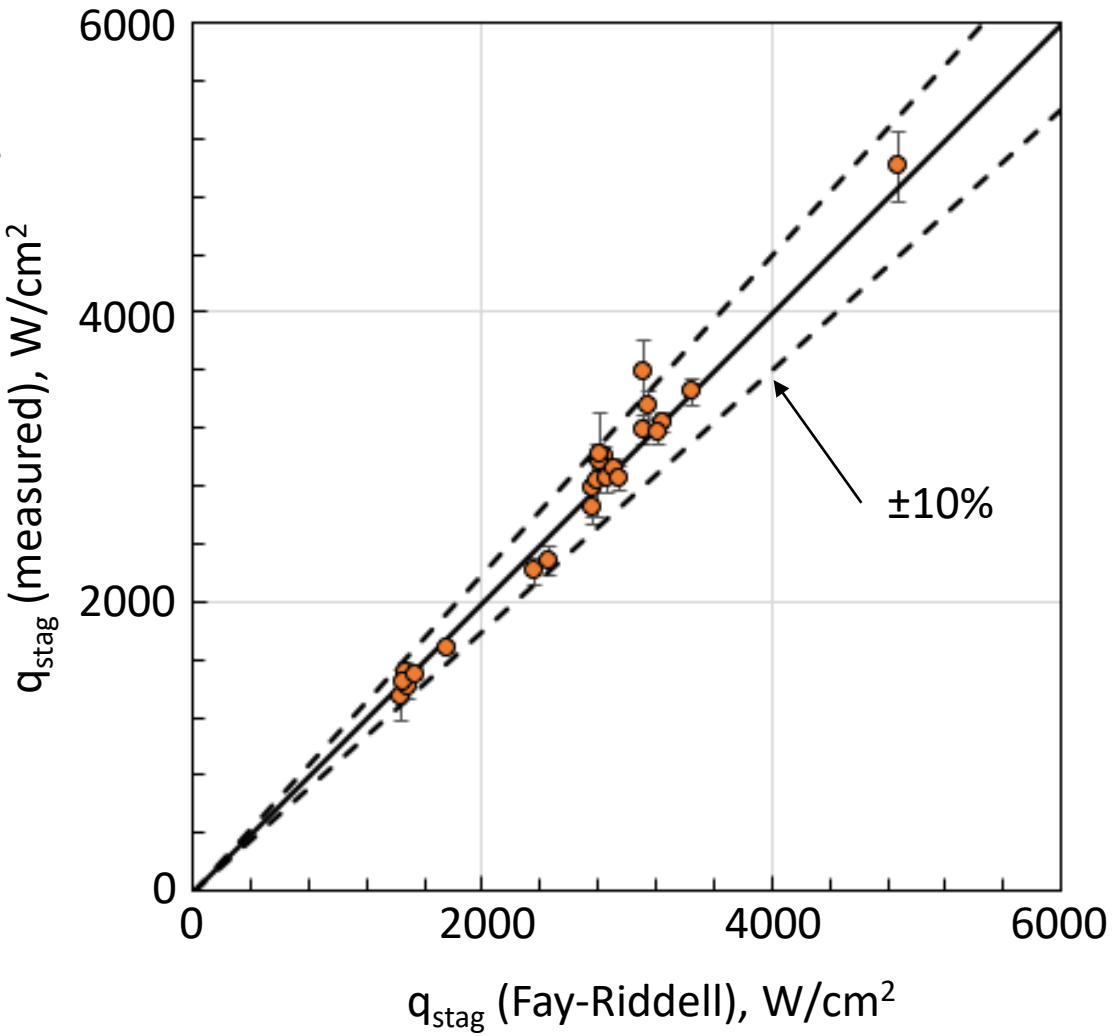

CFD Approach (Dinesh Prabhu)

- Computed using the Data Parallel Line Relaxation (DPLR) code
- Axisymmetric geometry
- 5-species chemically reacting gas model: N_2, O_2, NO, N, and O
- Thermal equilibrium (i.e., a single temperature)
- Wall was assumed to be fully catalytic to recombination of atomic species (N and O)
- Turbulent-flow computations employed the simple algebraic turbulence model of Baldwin and Lomax
- Roughness Reynolds number was calculated for each image using measured conditions (T_w, velocity, pressure, etc.)
  - $k^+ = u_{\tau_0} k/\nu_w$, where
    - k is the average roughness element height, and
    - $u_{\tau_0} = (\tau_w/\rho_w)^{1/2}$ is the friction velocity on a smooth wall

Results

- Heat-flux augmentation correlated with the roughness Reynolds number k^+ using the mean roughness element height, k
- Results were within the bounds of the PANT correlation* for sandgrain roughness

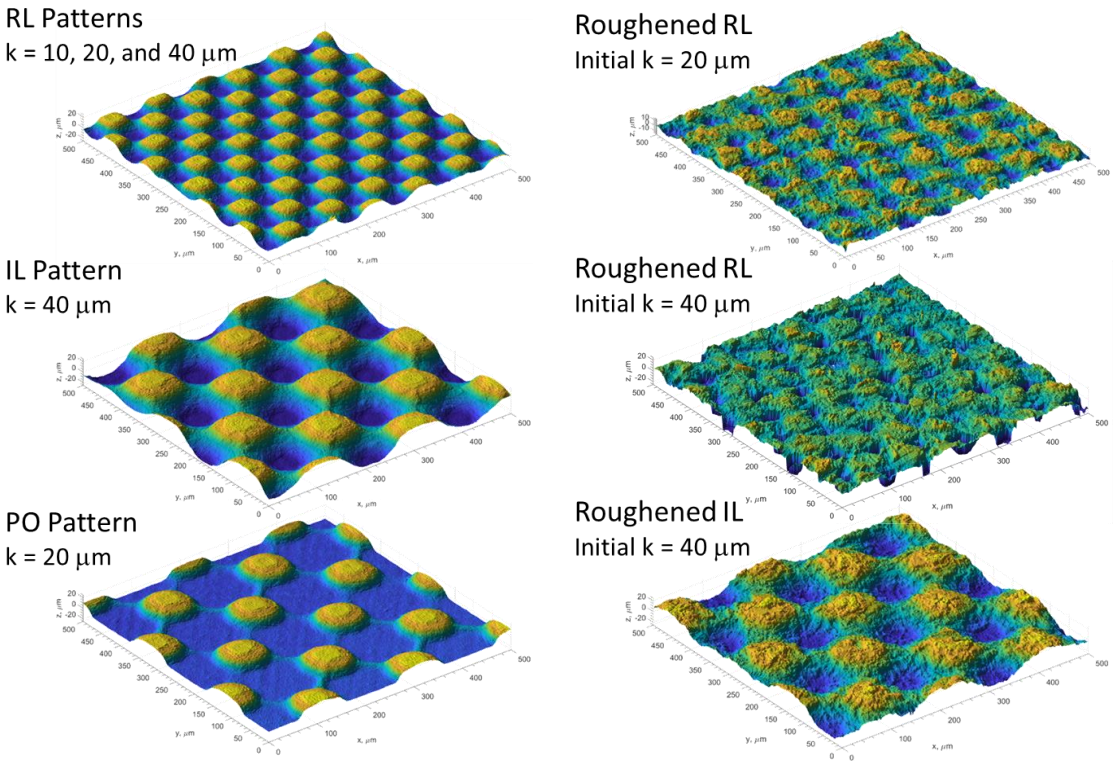

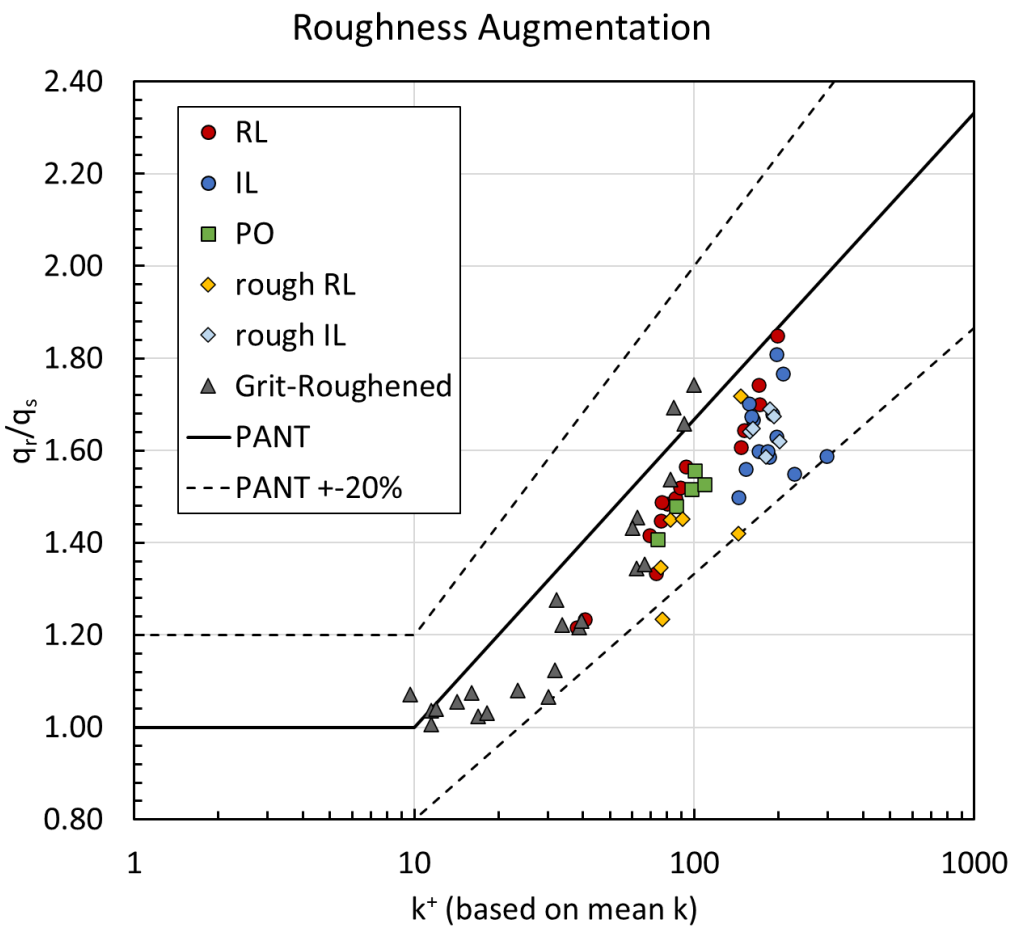

* Wool, M. R., "Final Summary Report Passive Nosetip Technology (PANT) Program," Aerotherm Report 75-159, June 1975.

Equivalent Sandgrain Models

- Several equivalent sandgrain roughness correlation have been considered
  - Dirling (1973) – includes supersonic boundary-layer data
    - "A Method for Computing Roughwall Heat Transfer Rates on Reentry Nosetips," AIAA Paper 73-763
    - Includes a roughness-element shape (bluntness) and spacing parameter
  - van Rij, *et al*. (2002) - includes supersonic boundary-layer data
    - "Analysis and Experiments on Three-Dimensional, Irregular Surface Roughness," Journal of Fluids Engineering, Vol. 124, No. 3, 2002
    - Includes a roughness-element shape (bluntness) and spacing parameter
    - 3D extension of Sigal and Danberg (1990)
  - Forooghi, et al. (2017) – subsonic data
    - "Toward a Universal Roughness Correlation," Journal of Fluids Engineering, December 2017
    - Based on RMS and skewness and includes a gradient parameter for bluntness
  - Flack, et al. (2010 and 2020) – subsonic data
    - "Review of Hydraulic Roughness Scales in the Fully Rough Regime," Journal of Fluids Engineering, 2010
    - "Skin Friction Measurements of Systematically-Varied Roughness: Probing the Role of Roughness Amplitude and Skewness," Flow, Turbulence and Combustion (2020)
    - Simplest form based on RMS, but can use skewness as well
  - Simmons, et al. (2022) – supersonic boundary layer data
    - "Characterizing Surface Roughness Effects through Direct Skin Friction Measurements," AIAA 2022-3925
    - Similar to Flack and Schultz (2010) but does not include skewness
    - Limited data set, but correlates boundary-layer profiles and direct skin friction measurements

Equivalent Sandgrain Models

- Several equivalent sandgrain roughness correlation have been considered
  - Dirling (1973) – includes supersonic boundary-layer data
    - "A Method for Computing Roughwall Heat Transfer Rates on Reentry Nosetips," AIAA Paper 73-763
    - Includes a roughness-element shape (bluntness) and spacing parameter
  - van Rij, *et al*. (2002) - includes supersonic boundary-layer data
    - "Analysis and Experiments on Three-Dimensional, Irregular Surface Roughness," Journal of Fluids Engineering, Vol. 124, No. 3, 2002
    - Includes a roughness-element shape (bluntness) and spacing parameter
    - 3D extension of Sigal and Danberg (1990)

Take into account bluntness and spacing but give an equivalent sandgrain roughness that is very large for the RL40 (40 μm) roughness elements and very small (hydraulically smooth) for the RL10 (10 μm) roughness elements.

Equivalent Sandgrain Models

- Several equivalent sandgrain roughness correlation have been considered

Rely on global parameters like the RMS(z) = S_q and/or the skewness, which are strongly dependent on the location of the mean surface (z = 0).

- Forooghi, et al. (2017) – subsonic data
  - "Toward a Universal Roughness Correlation," Journal of Fluids Engineering, December 2017
  - Based on RMS and skewness and includes a gradient parameter for bluntness
- Flack, et al. (2010 and 2020) – subsonic data
  - "Review of Hydraulic Roughness Scales in the Fully Rough Regime," Journal of Fluids Engineering, 2010
  - "Skin Friction Measurements of Systematically-Varied Roughness: Probing the Role of Roughness Amplitude and Skewness," Flow, Turbulence and Combustion (2020)
  - Simplest form based on RMS, but can use skewness as well
- Simmons, et al. (2022) – supersonic boundary layer data
  - "Characterizing Surface Roughness Effects through Direct Skin Friction Measurements," AIAA 2022-3925
  - Similar to Flack and Schultz (2010) but does not include skewness
  - Limited data set, but correlates boundary-layer profiles and direct skin friction measurements

Equivalent Sandgrain Models

Surface	k_m (μm)	Dirling	van Rij	Forooghi 2017, Eqn. 15	Forooghi 2017, Eqn. 16	Flack 2020 (no skewness)	Flack 2020	Flack 2010	Simmons, 2022
RL10	10.25	0.39	1.17	15.37	20.26	6.29	17.37	22.24	13.11
RL20	19.81	10.69	21.77	31.69	38.67	12.37	17.27	29.06	25.79
RL40	42.80	265.22	82.81	56.73	54.94	26.71	27.83	29.42	55.69
IL	39.33	18.20	34.48	43.08	48.23	24.47	24.30	37.85	51.02
PO	20.41	0.91	3.24	35.51	22.18	4.95	53.14	40.19	10.32
								166.07	42.45

or, depending on were you place z = 0

National Aeronautics and
Space Administration

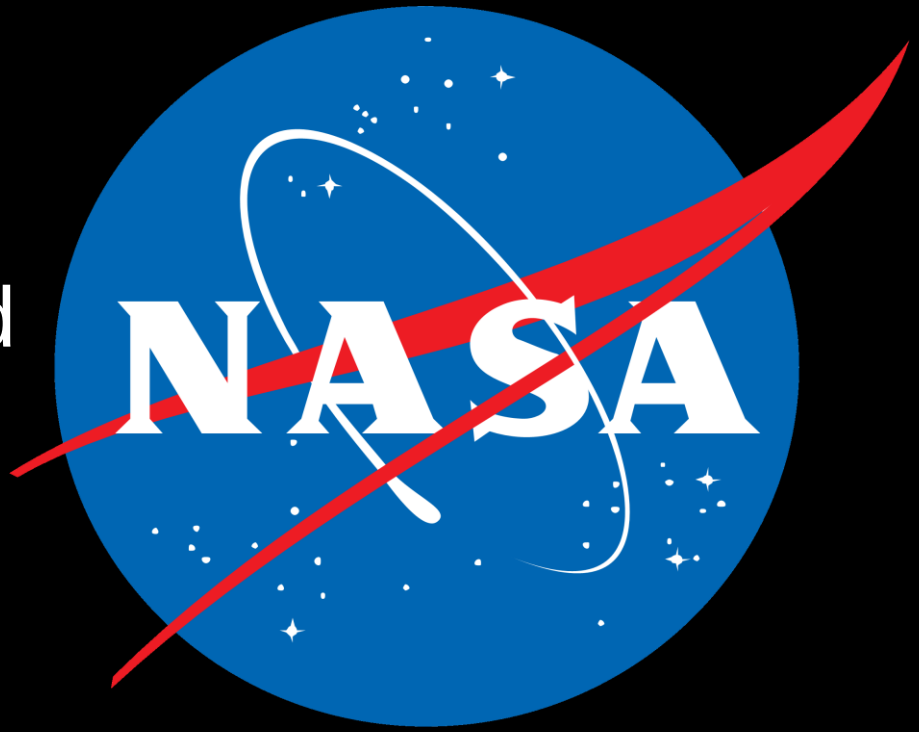

Ames Research Center
Entry Systems and Technology Division

Pattern Alignment

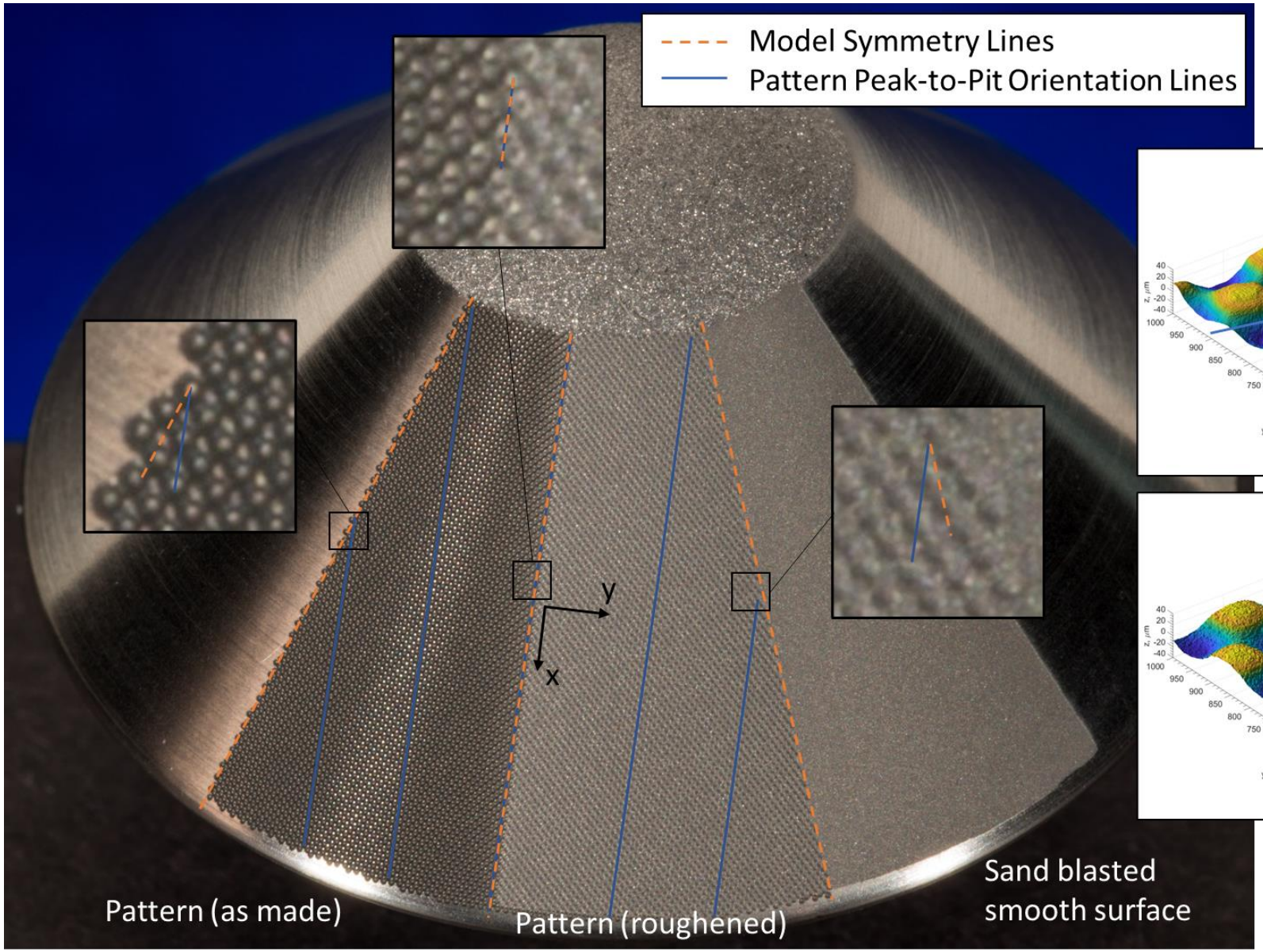

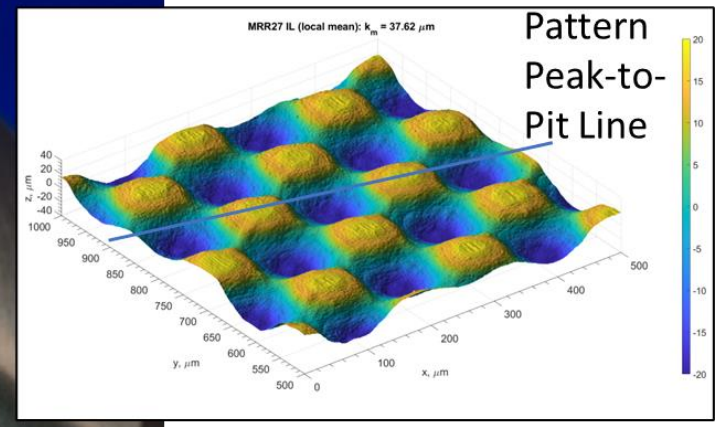

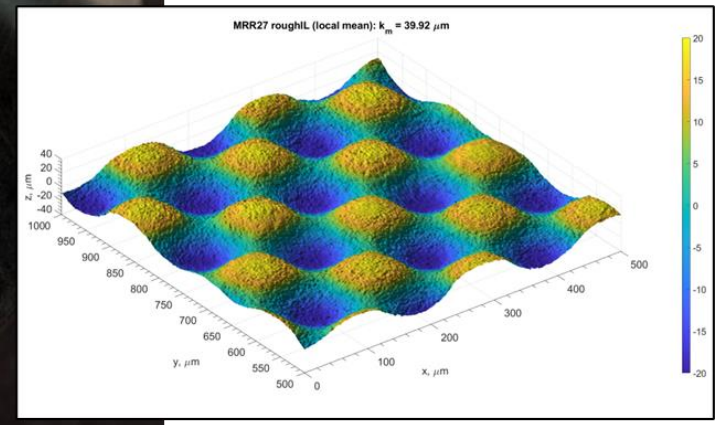

Effects of surface roughness

- Promote boundary-layer transition to turbulent flow
- Augment convective surface heating
  - "State of the Art" is the correlation of Powars
    - Data from the Passive Nosetip Technology (PANT) Program (c. 1970s)
    - Roughness produced by sand-blasting the models
    - Turbulent heat transfer augmentation correlates with the smooth-wall turbulent roughness Reynolds number, k^+

$$k^+ = u_{\tau_0} k / \nu_w$$

k is the average sand roughness element size

u_{τ_0} is the friction velocity

ν_w is the kinematic viscosity

Effect of Sand Roughness on Turbulent Heat Transfer
Passive Nosetip Technology (PANT) Program*

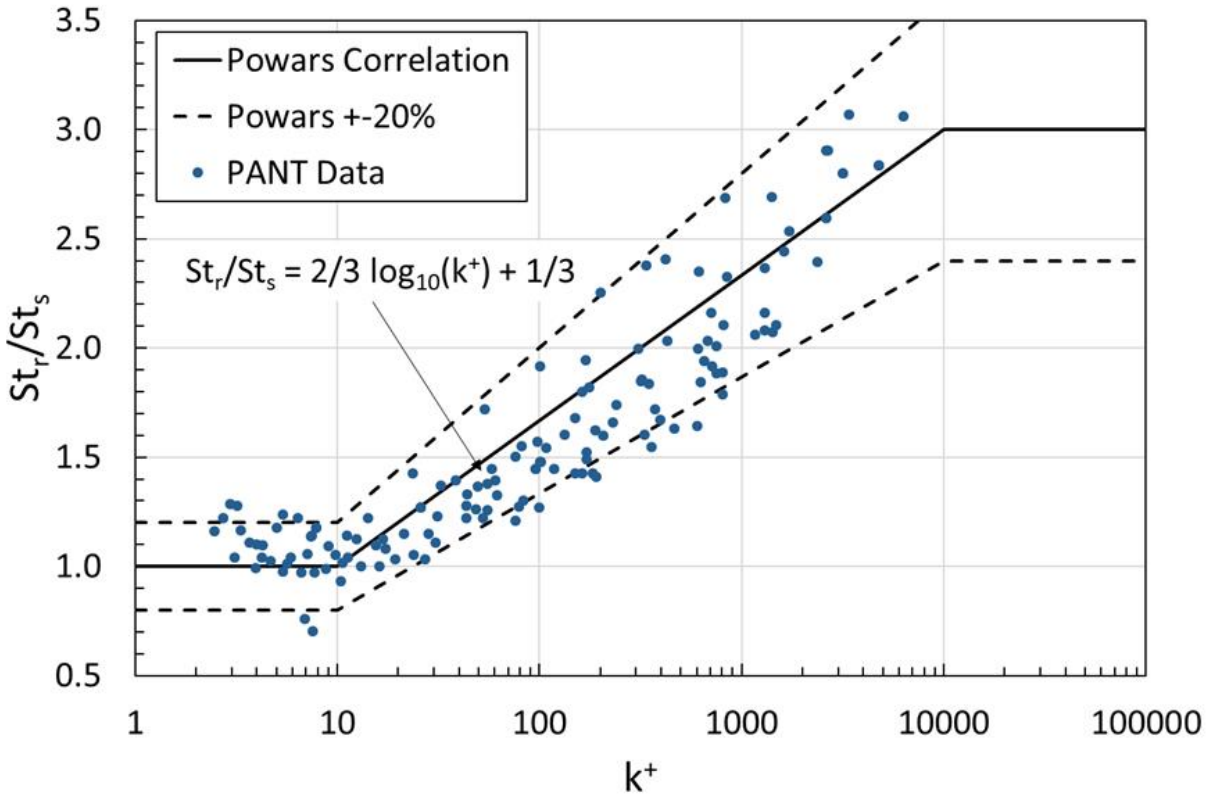

* Wool, M. R., "Final Summary Report Passive Nosetip Technology (PANT) Program," Aerotherm Report 75-159, June 1975.

Smooth-Wall Measurements

- Smooth wall reference measurements
  - Laminar measurement was made in a previous test campaign (single shot)
  - Turbulent data is from this campaign
    - Symbols are the average and 3σ of all eight shots
    - Profile for each taken at center of the wide smooth band, average over 20º of circumference
    - Nose caps were rough, to trip the flow